

PVP2008-61345

**LOOSENING RESISTANCE EVALUATION OF DOUBLE-NUT TIGHTENING
METHOD, SPRING WASHERS, AND CONICAL SPRING WASHERS;
FINITE ELEMENT STUDY**

**Takashi Yokoyama / Department of Mechanical Engineering,
The University of Tokyo, Tokyo, Japan
E-mail: yokoyama.takashi@fml.t.u-tokyo.ac.jp**

**Satoshi Izumi /
Department of Mechanical Engineering,
The University of Tokyo, Tokyo, Japan**

**Shinsuke Sakai /
Department of Mechanical Engineering,
The University of Tokyo, Tokyo, Japan**

ABSTRACT

The mechanisms of loosening resistance components are investigated within the framework of the three-dimensional finite element method (FEM). Here, the results of the double-nut tightening method (DN), spring washers (SW), and conical spring washers (CSW) are shown. This paper focuses on the comparison among the components above based on the results that have been published separately. For details on each analysis, readers are referred to [10-12].

We have found that DN shows significant loosening resistance if the locking is properly realized in the tightening process. However, if the locking is not performed properly, its ability to resist loosening completely disappears. SW shows negative loosening resistance because the sticking area on the contact surfaces is limited to two corner edges of the SW and the rotational force around these edges thus drastically leads to loosening. In regard to CSW, in the case of high axial force, it shows no apparent effect on preventing loosening. On the other hand, in the case of low axial force, it shows two opposite effects. The negative effect is an increase in the loosening rotation angle, while the positive one is the prevention of a decrease in axial force. When complete bearing-surface slip occurs, a CSW can prevent loosening because the positive effect becomes larger than the negative one. However, when only small bearing-surface slip occurs, a CSW cannot prevent loosening because the negative effect cancels the positive one.

INTRODUCTION

Bolted joints are widely used in mechanical structures due to the joints' ease of disassembly for maintenance and their relatively low cost. However, vibration-induced loosening due to dynamic loading has remained problematic, and fatal accidents due to joint loosening still frequently take place every year in Japan. As a response to these problems, several loosening resistance components have been developed and used. If the double-nut tightening method is applied according to the correct procedure, it is expected to have an effect on preventing loosening. However, if locking state is not properly achieved, this method does not show an effect. Although washers such as plain washers and spring washers also have been used in many industries in attempts to resist bolt loosening, it has been shown experimentally that their effect on preventing loosening rotation does not appear in every case [1-4].

Three-dimensional finite element models considering the helical profile specific to threads can represent the loosening of a bolted joint. In previous work [5], the authors performed FEM analysis on bolt loosening due to external loading perpendicular to the bolt axis (transverse loading) and obtained close qualitative agreement with the experimental results reported by Yamamoto et al. [6]. In addition, we investigated the mechanisms of a small degree of loosening rotation prior to the complete bearing-surface slip (loosening rotation due to micro bearing-surface slip) suggested by Kasei et al. [7] and Pai et al. [8] and showed that a small degree of loosening

occurs when the transverse load reaches about 50 % to 60 % of that of bearing-surface slip [9]. This modeling method using FEM enables us to examine the effects of loosening-resistance components on the prevention of loosening.

In the present study, the effects of the double-nut tightening method (DN) [10], a spring washer (SW) [11], and a conical spring washer (CSW) [12] on loosening resistance were investigated using the three-dimensional finite element modeling method. The loosening that accompanies the relative rotation of a bolt and a nut due to complete and micro bearing-surface slips is considered in this study. Based on our results, a guideline for choosing the proper loosening-resistance component is provided.

ANALYSIS METHOD

1. Overview of finite element model

A bolted joint is likely to loosen under transverse loading. In previous studies on bolt loosening under this condition, Junker's loosening apparatus, in which roller bearings are placed between a movable top plate and a fixed plate to minimize sliding friction, has been widely used to observe loosening behavior [13]. In the present study, we model a bolted joint employing a loosening-resistance component using Junker's loosening apparatus in order to examine the component's effects by observing the progress of loosening rotation and the decrease in axial force. The FEM model is shown in Fig. 1 and Fig. 2. We use ANSYS10.0, which is a general-purpose finite element method software. The model reproduces a helical profile of the internal and external threads, but detailed shapes such as the curvature of the bottom of the thread are not taken into account since a detailed evaluation of stress distribution is beyond the scope of the present study. The nominal size of the bolt and nut is M10, and the grade and position of the crossover is 6H/6g (expressed in terms of the Japanese Industrial Standards). Because the friction between the movable top plate and the fixed plate can be ignored in the loosening apparatus, only part of the movable plate is modeled, and the displacement of the bottom of the movable plate in the axial direction is fixed.

Contact elements are used to incorporate contact behavior at the interfaces such as the mating threads, the nut bearing surface, and so on. In this model created using ANSYS, the contact element pair TARGE170 and CONTA174, which realizes surface-surface contact between three-dimensional objects and which can deal with the Coulomb friction, is used. The pure penalty method is employed as a contact algorithm. To reduce calculation costs, axial force is generated by allowing initial interference between the movable plate and the lower nut (in the case of a DN joint) or the washer (in the case of SW and CSW joints). The transverse load is applied to the end surface of the movable plate as constrained displacement or force. A displacement-constrained boundary is employed in order to observe the loosening due to complete bearing-surface slip, while a force-constrained boundary is employed to

observe the loosening due to micro bearing-surface slip. The Young's modulus and Poisson's ratio for all the components (bolt, nut, SW, CSW, and movable top plate) are 205 GPa and 0.3, respectively. The friction coefficient of the contact surfaces is set to 0.15. The performed FEM analysis is quasi-static and elastic. Geometric nonlinearities are taken into account.

Detailed analysis conditions for each case of a DN joint, SW joint, and CSW joint are explained in the sections below. For each case, loosening progress is compared to the case of a conventional joint. The progress of loosening is observed from two viewpoints. One is the loosening rotation angle of the nut in relation to the torsion angle of the bolt (loosening rotation angle). The other is the decrease in axial force. Here, axial force means bolt tension.

2. Double-nut (DN) joint

Two methods are available to setup the double-nut joint, that is, the upper-nut rotation method and the lower-nut reverse rotation method. This study is intended for the latter. After the processes of lower-nut reverse rotation method, thread of the lower nut is in contact on the surface opposite to the one that is in contact in the standard tightening process. This state is called as locking state, and the force produced on the thread of lower nut is called as double-nut locking force. We have investigated the mechanism of the tightening processes elsewhere and obtained close agreements with experimental results [10]. Here, in order to reduce calculation costs, axial force and double-nut locking force are generated by using an initial interference scheme. The axial force and the double-nut locking force are generated by the interference between the movable plate and the lower nut and that between the upper nut and the lower nut, respectively. At the locking state, the lower surface of the lower-nut thread contacts the upper surface of the bolt thread. And the thread of the upper nut supports the axial force and double-nut locking force. Axial force is adjusted to 10 kN. Four kinds of locking states are employed. Case 1 has a high double-nut locking force of 8.8 kN, while Case 2 has a low double-nut locking force of 1.1 kN. Although Case 3 is in the locking state, its double-nut locking force is almost zero. Case 4 is not in the locking state, which means that there is a gap between the thread of the lower nut and that of the bolt. Therefore, the thread of the lower nut is not loaded at all and the thread of the upper nut supports the axial force. Loosening due to complete bearing-surface slip is investigated. The amplitude of the movable plates' transverse displacement is set to 0.3 mm. For details, readers are referred to [10].

3. Spring washer (SW) joint

The general-use SW categorized in JIS B1251 is modeled. In order to reproduce the spring force of a SW, the initial stress is applied to the flat C-shaped volume, which has a slit of 10 degrees. The detailed modeling process is described in Fig. 3. As shown in Fig. 3(a), while one end of the SW is fixed, the other end is displaced by 2.5 mm along the normal direction.

In the next step, the shape is updated by using a deformed shape and then all the stress is cleared (Fig. 3(b)). In step (c), the resulting updated shape is compressed so that its deformed shape becomes flat like the initial shape shown in Fig. 3(a). In step (d), all the resulting stress is output as initial stress. In step (e), the recorded initial stress is given to the initial flat C-shaped volume. The spring force becomes about 1 kN. Axial force is set to 10kN. Both complete and micro bearing-surface slips are investigated. In the former case, the amplitude of the movable plates' transverse displacement is set to 0.4 mm. Two vibration directions (x and z directions) are applied. For details, readers are referred to [11].

4. Conical spring washer (CSW) joint

The modeled CSW is classified as "1L" in JIS B1251. The deflection-force relationship is shown in Fig. 4. Its total deflection is 0.5 mm. Two kinds of axial force are applied; one is a low axial force (10 kN) in which the CSW is not fully compressed, and the other is a high axial force (20 kN) in which the CSW is fully compressed. Both complete and micro bearing-surface slips are investigated. In the former case, the amplitude of the movable plate is set to 0.3 mm in the case of low axial force (10 kN) and 0.4 mm in the case of high axial force (20kN). For details, readers are referred to [12].

ANALYSIS RESULTS AND DISCUSSION

1. DN joint [10]

The variations in axial force during three vibration cycles are shown in Fig. 5 (Cases 1 - 3) and Fig. 6 (Case 4). And the variations in double-nut locking force relative to the initial value are shown in Fig. 7 and Fig. 8, respectively. It is found that the variation in axial force shows a half-cycle period. In addition, it can be seen that the variation becomes large as the double-nut locking force becomes small. Judging from Fig. 7 and Fig. 8, it can be considered that the variation in axial force originates from the variation in double-nut locking force. In Case 4, although there is a gap between the thread of the lower nut and the bolt in its tightening process, it is found that double-nut locking force appears due to the applied vibration.

A significant decrease in axial force occurs only in Case 4. Even though complete bearing-surface slip occurs, there is no significant decrease in Cases 1 to 3. The amounts of the decrease in axial force during the third cycle are 0.65, 2.7, 4.7, and 220 N/cycle, respectively.

These results indicate that if the locking state is properly achieved, the double-nut tightening method significantly prevents loosening regardless of the magnitude of the locking force. However, if locking state is not properly achieved, the loosening resistance performance completely vanishes and loosening is increased to about twice as much as a conventional joint. This result agrees with Yamamoto's and Kasei's experiments [14].

2. SW joint loosening due to complete bearing-surface slip [11]

The loosening rotation angle during three vibration cycles is shown in Fig. 9. It is observed that the loosening rotation of the SW joint proceeds faster than that of the standard joint. It can be also said that there is no significant dependence on the vibration directions (x and z directions). Two effects are considered to increase loosening rotation. One is that the torsion of the bolt axis increases because the grip length of the joint is increased by adding a SW under the nut. The other is that the pressure distribution of a SW is concentrated on the corner edges. The details are discussed below.

The relationship of load and displacement (x -direction) are shown in Fig. 10. For comparison, that of a conventional joint is shown in Fig. 11. It is widely accepted that the load-displacement curve consists of three kinds of slopes: a steep-slope (A), a gradual-slope (B), and a flat slope (D). However, it can be seen that a low gradual-slope (C) appears in the SW model.

Images of the contact state during x -direction vibration are shown in Fig. 12. Symbols A to D correspond to those denoted in Fig. 10. First, in slope A, partial slip occurs both on the thread surface and on the SW surfaces. Secondly, in slope B, the entire thread surface undergoes complete slip. At the end of slope B, the stuck regions on the SW surfaces are concentrated around three or four edge points. Next, in slope C, the stuck regions are limited to only two edge points. The rotation of the SW around these stuck edge points occurs at this stage. Details of the mechanism of this rotation are discussed later. Finally, in the former part of slope D, complete slip occurs both on the thread surface and on the SW surfaces. In the latter part of slope D, the thread surface regains a sticking state.

The progress in the rotation angles of the nut and the SW in the case of x vibration are shown in Fig. 13. It is found that the rotation direction depends on the vibration direction. The SW rotates in the loosening direction during stage C of $+x$ displacement while it rotates slightly in the tightening direction during that of $-x$ displacement. This reverse rotation is caused by rotation around two edge points as illustrated in Fig. 14. Depending on the vibration direction, the rotation direction of the SW changes. Due to its effect, nut rotation during $+x$ displacement (around cycle 0, 1, 2) becomes larger than that in the $-x$ direction (around cycles 0.5, 1.5, and 2.5). Particularly, the nut rotation proceeds mainly during stage C while it does not proceed as much during stage D in which complete bearing-surface slip occurs. This indicated that the SW joint could loosen more than the conventional joint even prior to the load of complete bearing-surface slip.

3. SW joint loosening due to micro bearing-surface slip [11]

The rates of the loosening rotation angle under various transverse loads, which are less than critical for complete bearing-surface slip, are plotted in Fig. 15. Here, the transverse load F is normalized by the critical value F_{cr} . It is found the loosening rotations in the cases of SW are larger than that of a

conventional nut. The rate increases drastically around $F/F_{cr}=0.80$ ($F=1200$ N) in the case of the SW joint. This increase is caused by the rotation around the two stuck edge points, which are described in Fig 14.

4. CSW joint loosening due to complete bearing-surface slip [12]

The loosening rotation angle and the decrease in axial force during three vibration cycles are shown in Fig. 16. In the case of low axial force (10 kN) (Fig. 16(a)), it can be seen that the loosening rotation of the CSW joint proceeds faster than that of the standard joint. The loosening rotation angles during the third cycle of the CSW and standard joints are 0.26 deg and 0.21 deg, respectively. On the other hand, the decrease in axial force of the CSW joint proceeds slower than that of the standard joint. The decrease in axial force during the third cycle is 81 N for the CSW joint while it is 241 N for the standard joint.

Larger loosening rotation might be caused by changes in the distribution of contact pressure. The contact pressure between the nut bearing surface and the CSW, shown in the upper part of Fig. 17, is apparently concentrated around the inner diameter of the CSW, as compared with the standard joint shown in the lower part. The equivalent diameter of friction torque based on the pressure distribution of the CSW joint is estimated as 12.4mm while that of the standard joint is 14.6 mm (assuming uniform contact pressure distribution). To sum up, it can be said that loosening rotation in the CSW joint proceeds more quickly because of the smaller equivalent diameter of friction torque.

On the other hand, it is considered that the decrease in axial force depends on the compressing spring constant of the cramped component. When a bolted joint is tightened and the grip length is shortened by ε_c the generated axial force F_s is expressed as below using the compressing spring constant of cramped components C_c ,

$$F_s = C_c \varepsilon_c. \quad (1)$$

When the cramped components consist of two components whose compressing spring constants are C_1 and C_2 , C_c is expressed as

$$C_c = \frac{C_1 C_2}{C_1 + C_2}. \quad (2)$$

If C_1 is sufficiently smaller than C_2 , C_c can be approximated as

$$C_c \approx C_1. \quad (3)$$

As can be seen from Fig. 4, the deflection-force relation can be divided into two regions. One is the region below approximately 10 kN, where the axial force is sustained mainly

by the reaction force of the CSW spring. The other is over approximately 10 kN, where the CSW is fully compressed. The compressing spring constant of the CSW at 10 kN estimated from the curve in Fig. 4 is $1.29 \cdot 10^5$ N/mm while that of the cramped component, which is calculated using the expression proposed by LORI et al. [15], is estimated as $1.94 \cdot 10^6$ N/mm. Thus, the total compressing spring constant C_c is approximated as the spring constant of the CSW using expression (3). Because the smaller spring constant of the cramped components induces a slower decrease in axial force as can be seen in expression (1), the decrease in axial force proceeds slower in the CSW joint.

In the case of high axial force (20 kN) (Fig. 16(b)), both the loosening rotation angle and the decrease in axial force show similar behaviors, except for the initial drop in axial force in the case of the standard joint. These values are the same (0.36 deg) in the third cycle. According to the deflection-force relation of the CSW shown in Fig. 4, when the axial force reaches 20 kN, the macroscopic deflection of the CSW has already occurred and the entire interface is in a compression state. Thus, the contact pressure distribution between the nut-bearing surface and the CSW becomes more uniform and similar to that of the standard joint, as compared with the case of 10 kN shown in Fig. 17. This leads to the equal loosening behavior of the CSW joint and the standard joint in the case of high axial force (20 kN).

5. CSW joint loosening due to micro bearing-surface slip [12]

The relationships between a transverse load and the loosening rotation angle and that between a transverse load and a decrease in axial force are shown in Figs. 18 (a) and (b) in the case of low axial force (10 kN), and in Figs. 18 (c) and (d) in the case of high axial force (20 kN), respectively. Here, the transverse load F is normalized by the critical value F_{cr} . It is found that in the case of low axial force, the loosening rotation angle of the CSW joint becomes larger than that of the standard joint, as well as in the case of complete bearing-surface slip. However, the difference in the decrease in axial force becomes small. In the case of high axial force, those differences are negligibly small. The normalized critical transverse load required to induce small loosening (F/F_{cr}) ranges from 0.4 to 0.5 for all cases. It can be said that the CSW does not affect loosening.

6. Comparison of DN, SW, and CSW

On the basis of the results shown above, we discuss the comparison of loosening resistance components. It is clear that DN has the best loosening resistance performance among the three components. Even if the transverse load enough to cause complete bearing-surface slip is applied, loosening would be drastically suppressed by the DN. However, in actual tightening operation, the problem is a reliable control of locking state. To set up the locking state is not easy because serious control of the tightening torque is necessary in three

tightening processes; tightening of the lower nut, tightening of the upper nut, and rotating of the lower nut in the loosening direction.

On the contrary, such a troublesome problem does not take place in the SW and CSW tightening. However, as compared with DN, SW and CSW are not able to sufficiently suppress the loosening due to both bearing and thread surface slip. In particular, it should be noted that the SW induces significant loosening rotation prior to the bearing-surface slip. Thus we suggest that SW should not be used as a loosening resistance component without sufficient discussion. On the other hand, we can see that CSW provides a certain effect on the loosening resistance since it gives a higher spring force than SW and its spring force contributes to suppress the decrease in axial force during loosening. Therefore, it is expected that CSW shows better loosening resistance performance than SW.

CONCLUSION

Three-dimensional finite element analyses of M10 bolted joints using the double-nut tightening method (DN), a spring washer (SW), and a conical spring washer (CSW) subjected to a transverse load were performed and the loosening resistance performance of those components were investigated.

First, in regard to DN, the effect of the locking state on preventing loosening was clarified. We have found that DN shows significant loosening resistance if locking is properly achieved in its tightening process. However, if locking is not properly performed, its ability completely disappears.

Secondly, SW shows negative loosening resistance because the SW rotation occurs around two stuck edge points. Thus, the loosening rotation of the SW joint is increased drastically under the condition of micro bearing-surface slip. It can be concluded that using a SW is problematic from the point of view of loosening resistance.

Finally, regarding CSW, in the case of low axial force, under which a CSW is not fully compressed, two conflicting effects on loosening were seen. One is a negative aspect; that is, a CSW increases the loosening rotation angle due to the concentration of contact pressure around the inner diameter of bearing surface. The other is a positive one; that is, it prevents a decrease in axial force due to the smaller compressing spring constant compared to that of cramped component. The effect of a CSW on loosening is determined by the trade-off of these two effects. In the case of high axial force under which a CSW is fully compressed, the loosening rotation angle and the decrease in axial force do not depend on the use of a CSW.

ACKNOWLEDGMENTS

The primary author was supported through the 21st Century COE Program, "Mechanical Systems Innovation", by the Ministry of Education, Culture, Sports, Science and Technology-Japan.

REFERENCES

- [1] A. Yamamoto, S. Kasei, Evaluation of locking performance of threaded fastener locking devices by different types of thread-loosening tests (in Japanese), *Journal of the Japan Society of Precision Engineering*, 48, 6, (1982), pp. 801-806.
- [2] A. Yamamoto, S. Kasei, Comparative Evaluation of Threaded Fastener Locking Devices by Various Type Thread-Loosening Tests, *Bulletin of the Japan Society of Precision Engineering*, 15, 3, (1981), pp. 197-198.
- [3] T. Sakai, An enlarged edition: An outline of threaded fastening (in Japanese), Yokendo Ltd., Japan (2003), p. 133.
- [4] S. Kasei, T. Komura, S. Kanahara, J. Yamazaki, Bearing Surface Slip and Self-loosening of Threaded Fasteners (on Loosening Mechanism (4)) (in Japanese), *Proceedings of the Mechanical Engineering Congress*, Vol. 4, 07-1, (2007), pp. 59-60.
- [5] S. Izumi, T. Yokoyama, A. Iwasaki, S. Sakai, Three-dimensional Finite Element Analysis of Tightening and Loosening Mechanism of Threaded Fastener, *Engineering Failure Analysis*, 12, (2005), pp. 604-615.
- [6] A. Yamamoto, S. Kasei, Investigation on the Self-loosening of Threaded Fasteners under Transverse Vibration –A Solution for Self-loosening Mechanism– (in Japanese), *Journal of the Japan Society of Precision Engineering*, 43, 508, (1977), pp. 470-475.
- [7] S. Kasei, A Study of Self-Loosening of Bolted Joints Due to Repetition of Small Amount of Slippage at Bearing Surface, *Journal of Advanced Mechanical Design, Systems, and Manufacturing*, 1, 3, (2007), pp. 358-367.
- [8] N. G. Pai, D. P. Hess, Three-dimensional Finite Element Analysis of Threaded Fastener Loosening due to Dynamics Shear Load, *Engineering Failure Analysis*, 9, (2002), pp. 383-402.
- [9] S. Izumi, M. Kimura, S. Sakai, Small Loosening of Bolt-nut Fastener Due to Micro Bearing-Surface Slip: Finite Element Method Study, *Journal of Solid Mechanics and Materials Engineering*, 1, 11, (2007), pp. 1374-1384.
- [10] M. Kimura, S. Izumi, S. Sakai, Tightening and Self-loosening Behavior of Double-nut Tightening System by Three-dimensional Finite Element Method (in Japanese), *Transactions of the Japan Society of Mechanical Engineers, Series A*, 72, 719, (2006), pp. 967-973.
- [11] M. Kimura, S. Izumi, S. Sakai, Self-loosening Behavior of A Spring Washer: Three-dimensional Finite Element Method Study (in Japanese), *Transactions of the Japan Society of Mechanical Engineers, Series A*, 73, 734, (2007), pp. 1105-1110.
- [12] T. Yokoyama, K. Oishi, M. Kimura, S. Izumi, S. Sakai, Evaluation of Loosening resistance Performance of Conical Spring Washer by Three-dimensional Finite Element Analysis, *Journal of Solid Mechanics and Materials Engineering*, 2, 1, (2008), pp. 38-46.

[13] G. H. Junker, New Criteria for Self-Loosening of Fasteners Under Vibration, *SAE Transactions*, 78, (1969), pp. 314-335.
 [14] A. Yamamoto, The Proper Method of Double-nut

Fastening (in Japanese), *Science of Machine*, 38, 9, (1986), pp. 1023-1026.
 [15] A. Yamamoto, A theory and design of threaded fastening (in Japanese), Yokendo Ltd., Japan, (1995), p. 49.

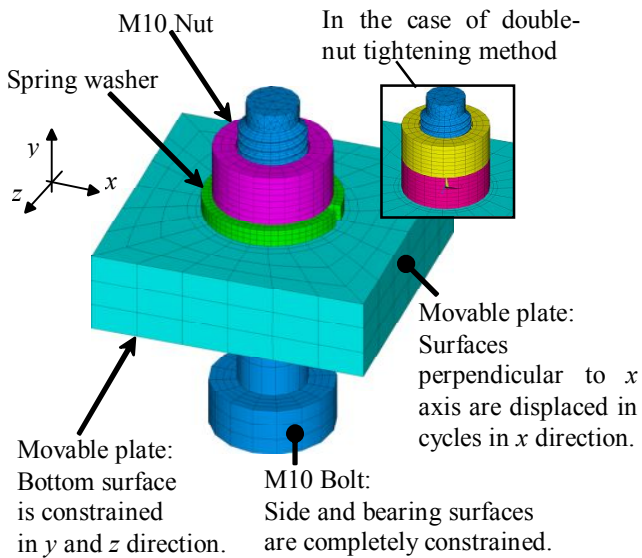


Fig. 1 Finite element model for loosening analysis of bolted joint

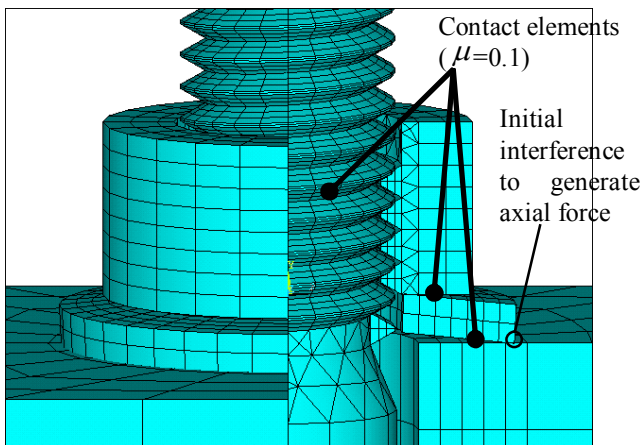


Fig. 2 Detail of thread part of FE model. (1/4 of nut, conical spring washer, and plate are visually removed in this figure.)

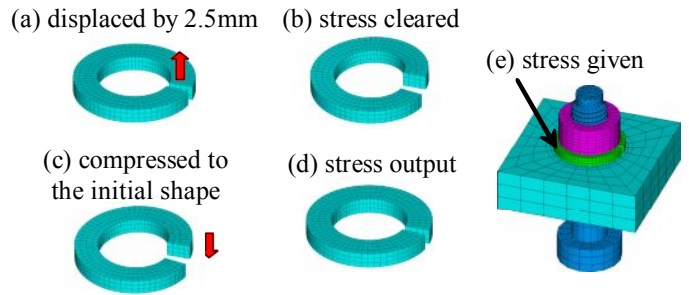


Fig. 3 Modeling Method for Spring Washer [11]

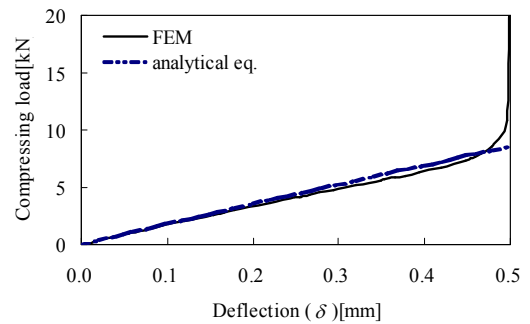


Fig. 4 Compressing property of conical spring washer [12]

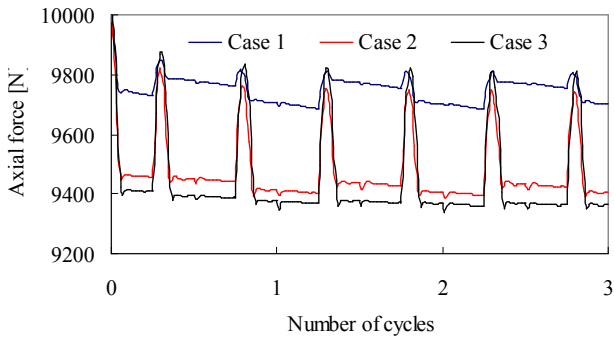


Fig. 5 Variations in axial forces (Case1 to Case3) [10]

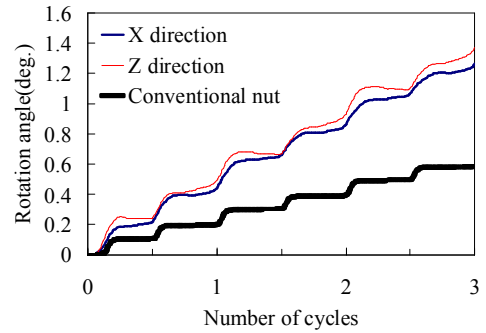


Fig. 9 Loosening rotation angle of the nut [11]

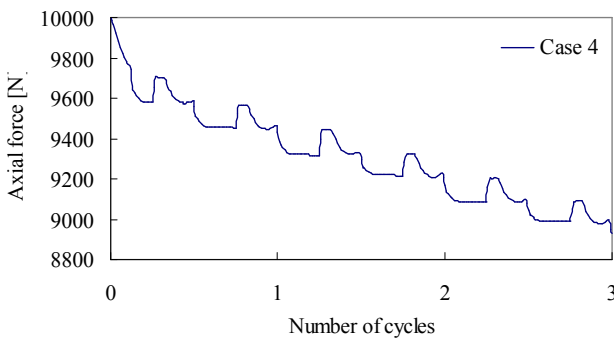


Fig. 6 Variation in axial force (Case4) [10]

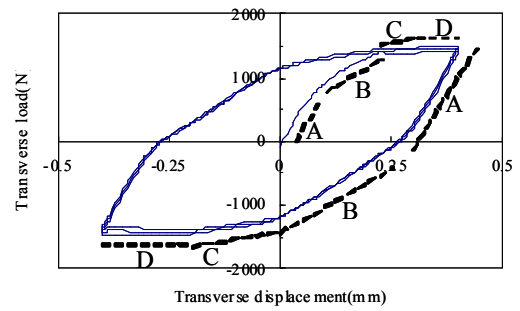


Fig. 10 Relationship between load and displacement. (With spring force) [11]

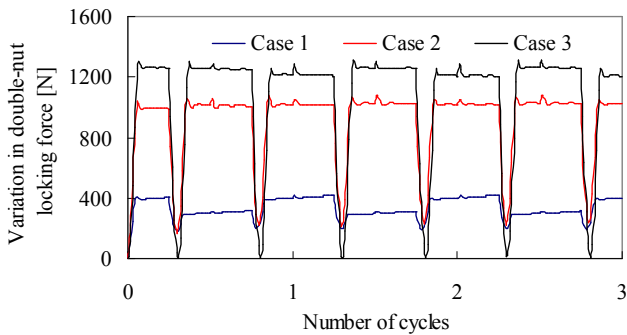


Fig. 7 Variations in double-nut locking forces (Case1 to Case3) [10]

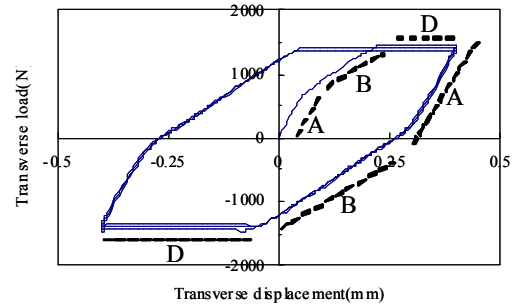


Fig. 11 Relationship between load and displacement. (Without spring force) [11]

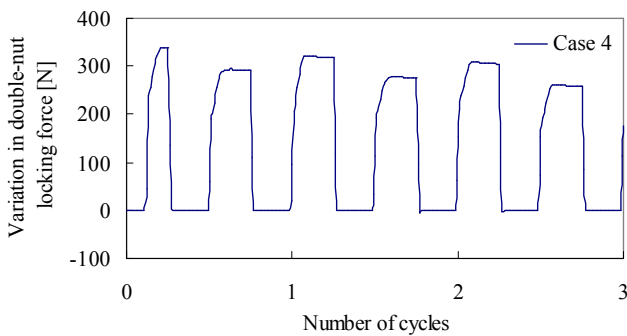


Fig. 8 Variation in double-nut locking force (Case4) [10]

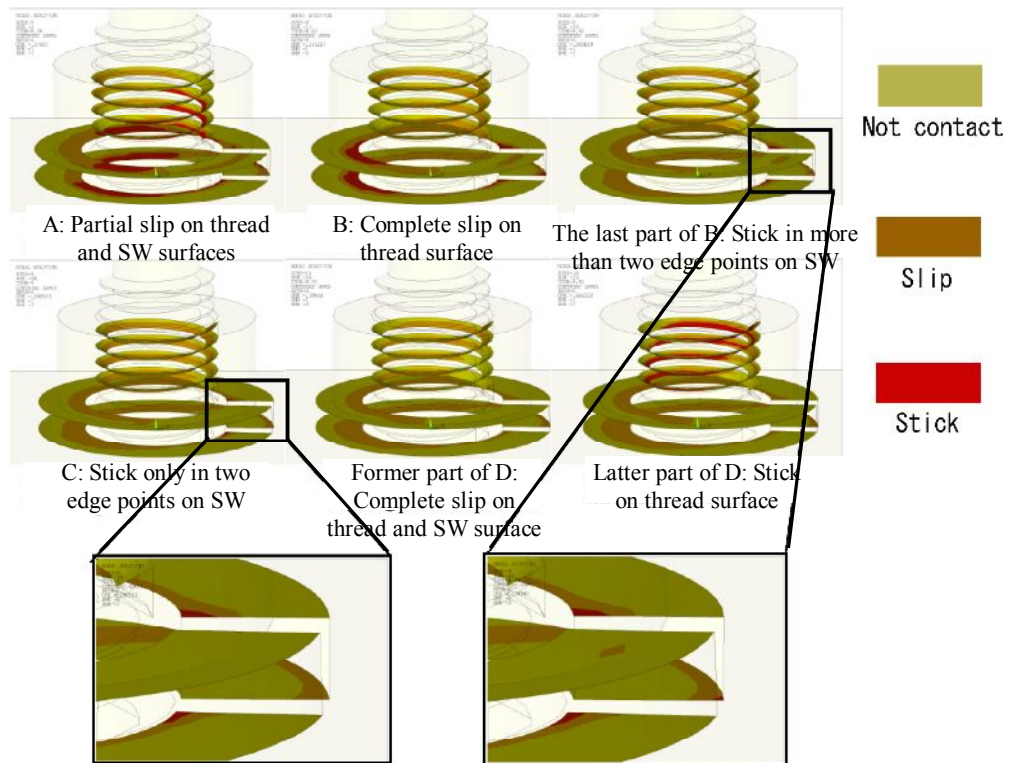


Fig. 12 Classification in contact states [11]

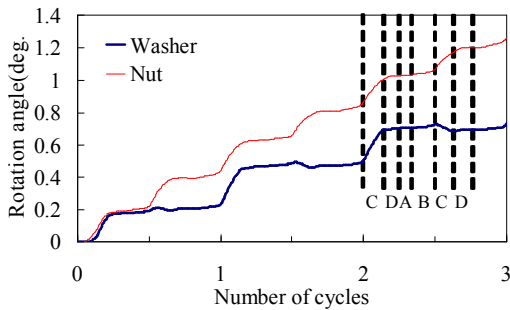


Fig. 13 Loosening rotation angle of the spring washer [11]

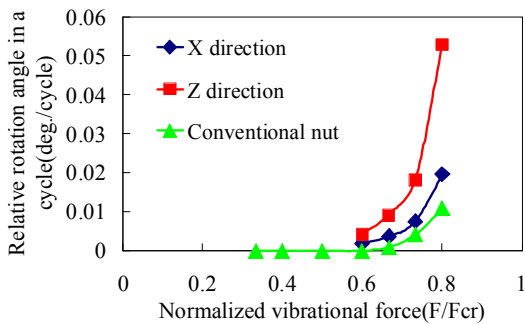


Fig. 15 Dependences of loosening rate on normalized vibration force [11]

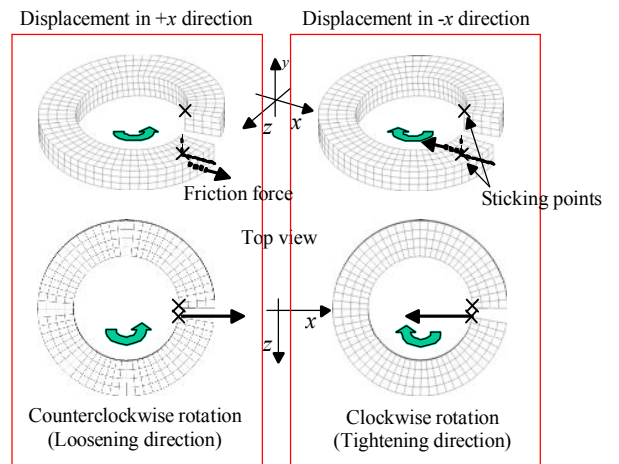
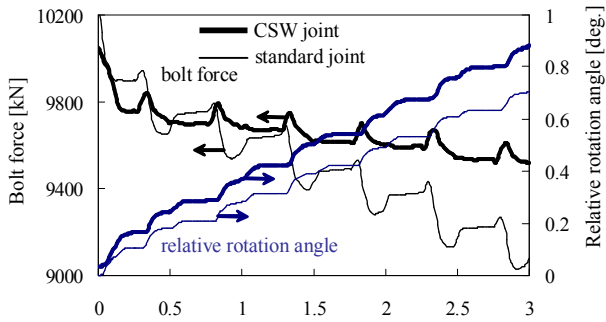
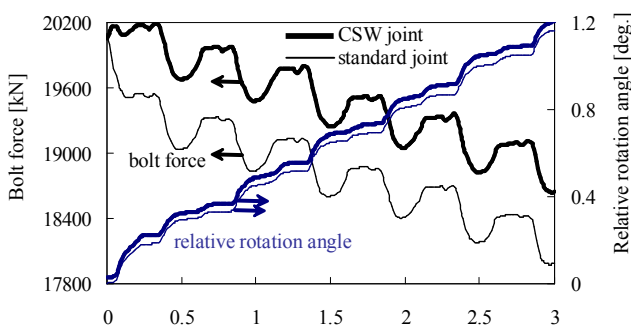


Fig. 14 Schematic illustrations of washer rotation during C state [11]



(a) Case of low axial force (10kN)



(b) Case of high axial force (20kN)

Fig. 16 Variation in loosening rotation angle and bolt force in the case of (a) low axial force (10kN) and (b) high axial force (20kN) [12]

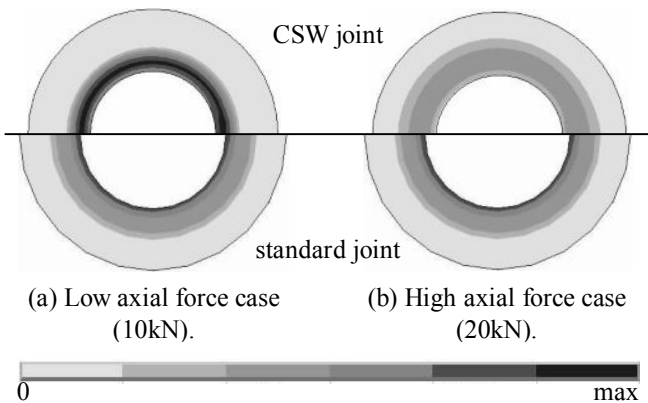
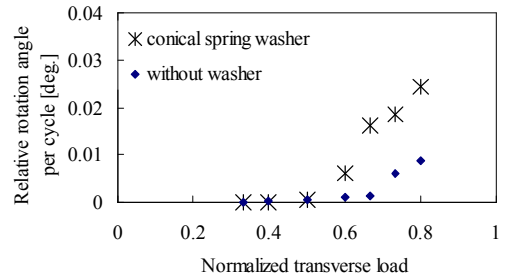
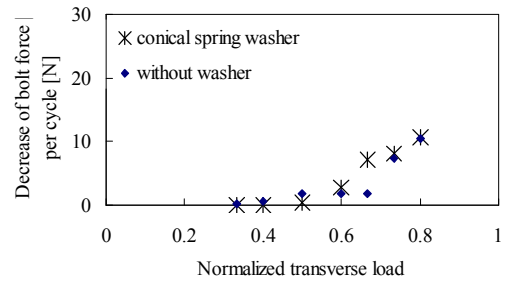


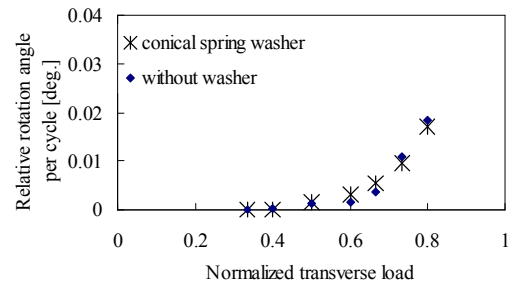
Fig. 17 Pressure distribution on nut bearing surface after axial force is applied [12] (max is 200MPa for (a), 400MPa for (b))



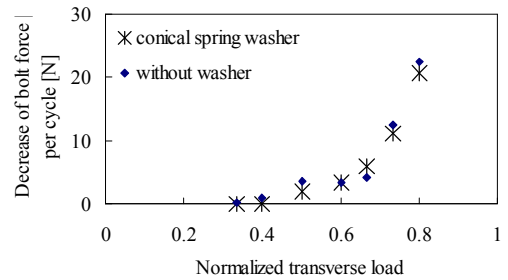
(a) Relation between loosening rotation angle and transverse load in the case of low axial force (10kN)



(b) Relation between decrease of bolt force and transverse load in the case of low axial force (10kN)



(c) Relation between loosening rotation angle and transverse load in the case of high axial force (20kN)



(d) Relation between decrease of bolt force and transverse load in the case of high axial force (20kN)

Fig. 18 Dependence of loosening rate on normalized transverse load [12]